Biochemical Pharmacology 81 (2011) 432–441

Contents lists available at ScienceDirect

Biochemical Pharmacology

journal homepage: www.elsevier.com/locate/biochempharm

The role of CYP3A4 in amiodarone-associated toxicity on HepG2 cells

Anja Zahno [a,b,c], Karin Brecht [a,b], Réjane Morand [a,b], Swarna Maseneni [a,b], Michael Török [a,b], Peter W. Lindinger [a,b,c], Stephan Krähenbühl [a,b,c,*]

[a] Division of Clinical Pharmacology & Toxicology, University Hospital, 4031 Basel, Switzerland
[b] Department of Biomedicine, University Hospital, 4031 Basel, Switzerland
[c] Swiss Centre of Applied Human Toxicology (SCAHT), University Hospital, 4031 Basel, Switzerland

ARTICLE INFO

Article history:
Received 24 August 2010
Accepted 2 November 2010

Keywords:
Amiodarone
N-mono-desethylamiodarone
N-di-desethylamiodarone
HepG2 cells
CYP3A4

ABSTRACT

Amiodarone is a class III antiarrhythmic drug with potentially life-threatening hepatotoxicity. Recent *in vitro* investigations suggested that the mono-N-desethyl (MDEA) and di-N-desethyl (DDEA) metabolites may cause amiodarone's hepatotoxicity. Since cytochrome P450 (CYP) 3A4 is responsible for amiodarone N-deethylation, CYP3A4 induction may represent a risk factor. Our aim was therefore to investigate the role of CYP3A4 in amiodarone-associated hepatotoxicity. First, we showed that 50 μM amiodarone is more toxic to primary human hepatocytes after CYP induction with rifampicin. Second, we overexpressed human CYP3A4 in HepG2 cells (HepG2 cells/CYP3A4) for studying the interaction between CYP3A4 and amiodarone in more detail. We also used HepG2 wild type cells (HepG2 cells/wt) co-incubated with human CYP3A4 supersomes for amiodarone activation (HepG2 cells/CYP3A4 supersomes). Amiodarone (10–50 μM) was cytotoxic for HepG2 cells/CYP3A4 or HepG2 cells/CYP3A4 supersomes, but not for HepG2 cells/wt or less toxic for HepG2 cells/wt incubated with control supersomes without CYP3A4. Co-incubation with ketoconazole, attenuated cytotoxicity of amiodarone incubated with HepG2 cells/CYP3A4 or HepG2 cells/CYP3A4 supersomes. MDEA and DDEA were formed only in incubations containing HepG2 cells/CYP3A4 or HepG2 cells/CYP3A4 supersomes but not by HepG2 cells/wt or HepG2 cells/wt with control supersomes. Metabolized amiodarone triggered the production of reactive oxygen species, induced mitochondrial damage and cytochrome *c* release, and promoted apoptosis/necrosis in HepG2 cells/CYP3A4, but not HepG2 cells/wt. This study supports the hypothesis that a high CYP3A4 activity is a risk factor for amiodarone's hepatotoxicity. Since CYP3A4 inducers are used frequently and amiodarone-associated hepatotoxicity can be fatal, our observations may be clinically relevant.

1. Introduction

Amiodarone (2-*n*-butyl-3-[3,5 diiodo-4-diethylaminoethoxy-benzoyl]-benzofuran) is a class III antiarrhythmic drug with additional classes I and II properties used in the treatment of a wide spectrum of cardiac arrhythmias [1]. Amiodarone's therapeutic use is limited because of its numerous side effects that include thyroidal [2], pulmonary [3,4], ocular [5] and/or liver toxicity [6–8]. Amiodarone is a mitochondrial toxicant associated with uncoupling of oxidative phosphorylation and inhibition of the electron transport chain and β-oxidation of fatty acids [9–13]. The mechanisms leading to the toxicity of amiodarone are not completely understood, but most likely involve tissue accumulation of the parent compound as well as of metabolites, eventually resulting in cellular and organ toxicity due to impaired mitochondrial function [13,14]. Amiodarone is metabolized to mono-N-desethylamiodarone (MDEA) [15] and di-N-desethylamiodarone (DDEA) [16] by N-deethylation by cytochrome P450 (CYP) 3A4. We have shown previously that MDEA and DDEA are strong inhibitors of the respiratory chain and are both associated with ROS production [13]. Moreover, we suggested that these metabolites are at least partially responsible for the hepatic toxicity in patients treated with amiodarone. Therefore, we hypothesized that induction of cytochrome P450 (CYP) 3A4, the main CYP isoenzyme responsible for amiodarone deethylation [17], may be a risk factor for hepatotoxicity associated with amiodarone. Since CYP3A4 inducers (e.g. antiepileptics such as phenytoin, phenobarbital and carbamazepine as well as rifampicin and efavirenz) are used frequently and amiodarone-mediated hepatotoxicity is potentially fatal [7], improved knowledge about the cellular mechanisms of amiodarone hepatotoxicity appears to be important to manage patients treated with this drug.

In order to reach our aim, we established and characterized stably transduced cells overexpressing human CYP3A4 using the

* Corresponding author at: Clinical Pharmacology & Toxicology, University Hospital, CH-4031 Basel, Switzerland. Tel.: +41 61 265 4715; fax: +41 61 265 4560.
E-mail address: kraehenbuehl@uhbs.ch (S. Krähenbühl).

0006-2952/$ – see front matter © 2010 Elsevier Inc. All rights reserved.
doi:10.1016/j.bcp.2010.11.002

hepatocyte cell line HepG2 (HepG2 cells/CYP3A4). This system allowed us to investigate the metabolism of amiodarone and the generation of the two toxic metabolites MDEA and DDEA within the cells. For comparison, we also employed a system with extracellular generation of the amiodarone metabolites consisting of HepG2 wt cells (HepG2 cells/wt) co-incubated with human CYP3A4 supersomes (HepG2 cells/CYP3A4 supersomes). Using these two systems, we could study the importance of the amiodarone N-desethyl metabolites for cytotoxicity associated with amiodarone in detail.

2. Materials and methods

2.1. Material

Amiodarone, mono-N-desethylamiodarone and L8040 (HPLC internal standard, IS) were purchased from Sanofi Recherche (Brussels, Belgium). Human CYP3A4 supersomes with supplementation of cytochrome b_5 and P450 reductase and insect cell control supersomes without CYP3A4 activity were from BD Gentest (Woburn, MA, USA). Cell culture supplements were purchased from GIBCO (Paisley, UK). Cell culture plates were purchased form BD Bioscience (Franklin Lakes, NJ). NADPH was obtained from Sigma–Aldrich (Switzerland) and the ToxiLight® BioAssay Kit from Lonza (Basel, Switzerland). Methanol LiChrosolv for HPLC use was from Merck (Darmstadt, Germany). All other chemicals used were purchased from Sigma or Fluka (Buchs, Switzerland).

2.2. Cell lines and cell culture

Cryo-preserved primary human hepatocytes (BD Gentest, Woburn, MA, USA) were recovered using the manufacturer's protocol and cultured for 24 h before the addition of drugs.

The hepatocyte cell line HepG2 was provided by Professor Dietrich von Schweinitz (University Hospital Basel, Switzerland). HepG2 wild type cells (HepG2 cells/wt), GFP cells (vector control) and HepG2 cells overexpressing human CYP3A4 (HepG2 cells/CYP3A4) were cultured in Dulbecco's modified Eagle's medium (DMEM; with 2 mmol/l GlutaMAX®, 1.0 g/l glucose and sodium bicarbonate) supplemented with 10% (v/v) heat-inactivated fetal calf serum, 10 mM HEPES buffer, pH 7.2 and non-essential amino acids. The culture conditions were 5% CO_2 and 95% air atmosphere at 37 °C.

2.3. Construction of the expression vector pCR2.1-CYP3A4

The coding region sequence of human CYP3A4 was obtained from NCBI's nucleotide sequence database (Ref Seq NM_017460). cDNA was generated by RT-PCR from RNA extracted from human liver with the use of the SuperScript™III RT-PCR kit (Invitrogen, Basel, Switzerland) according to the manufacturer's recommendations. The following forward and reverse oligonucleotide sequences were used: forward 5′-TGATGCTCTCATCCCAGACTTGG-3′ and reverse 5′-TCAGGCTCCACTTAGGTGCA-3′. The amplified product was cloned into the pCR®2.1-TOPO® vector (Invitrogen, Basel, Switzerland).

2.4. Production of lentivectors and transduction of HepG2 cells

The 1513-bp fragment containing the human CYP3A4 complete coding sequence was excised from the pCR®2.1-TOPO® vector and subcloned into the lentiviral pWpiresGFP vector. The vector envelope plasmid pMD2G, the packaging plasmid pCMCΔR8.91 and the pWpiresGFP vector were kindly provided by Dr. Didier Trono (University of Geneva, Switzerland). For the production of virions, pMD2G, pCMCΔR8.91 and the vector pWPhCYP3A4iresGFP (or empty vector pWpiresGFP) were transfected into 293T cells by calcium phosphate precipitation as described elsewhere [18]. Twelve hours after transfection, the medium was replaced. The virus containing supernatant was harvested at 38 h post transfection, filtered and stored at −70 °C.

2.5. Expression of human CYP3A4 in HepG2 cells

HepG2 cells (0.5×10^5) were seeded in six-well plates and incubated with viral supernatant (prepared as described above) in the presence of Polybrene® (Aldrich, Buchs, Switzerland). The success of transduction was assessed by fluorescence-activated cell sorting (FACS) analysis. Cells expressing green fluorescent protein (EGFP) were separated and passaged. Expression of human CYP3A4 in the transduced HepG2 cells was determined with quantitative real-time PCR (QPCR). Total RNA was isolated using the RNeasy® (Qiagen, Basel, Switzerland) kit according to the manufacturer's recommendations. Superscript™II in combination with oligo (dT) and Random Hexamer primers (Gibco BRL, Basel, Switzerland) was used for reverse transcription of 2 μg total RNA. Quantification was performed on an ABI PRISM 7700 Sequence Detector (PE Biosystems, Rotkreuz, Switzerland). Reporter probes hCYP3A4 (5′-AGGAGAGAACACTGCTCGTGGTTTCACAG-3′) and GAPDH (5′-CGCCTGGTCACCAGGGCTGC-3′) FAM/TAMRA were from Eurogentec (Seraing, Belgium); the hCYP3A4 (forward: 5′-GATTGACTCTCAGAATTCAAAAGAAACTGA-3′; reverse: 5′-GGTGAGTGGCCAGTTCATACATAA-3′) and GAPDH (forward: 5′-GGTGAAGGTCGGAGTCAACG-3′; reverse: 5′-ACCATGTAGTTGAGGTCAATGAAG-3′) forward and reverse primers were from Microsynth (Balgach, Switzerland).

2.6. Human CYP3A4 protein expression in HepG2 cells overexpressing CYP3A4 (HepG2 cells/CYP3A4)

CYP3A4 expression was checked by Western blotting using a polyclonal hCYP3A4 antibody (Daiichi Pure Chemicals, Tokyo, Japan). Cells (10^6) were harvested using lysis buffer (1% NP-40 [Nonidet P-40], 50 mM Tris, pH 7.5, 150 mM NaCl) and a protease inhibitor cocktail (Roche AG, Basel, Switzerland) plus 1 mM PMSF (phenylmethylsulfonyl fluoride). Proteins were separated by electrophoresis in the presence of molecular weight standards (Gibco, Paisly, UK) on a 10% polyacrylamide sodium dodecyl sulfate (SDS) gel and transferred onto a nitrocellulose membrane (BioradTrans-Blot, Hercules, USA). Membranes were first incubated with the 1/500 diluted goat anti-human CYP3A4 antibody. A secondary peroxidase-conjugated anti-goat antibody (Jackson Laboratories Inc., Sacramento, CA, USA) was used for chemiluminescence detection (ECL, Amersham International, Little Chalfont, UK) according to the manufacturer's protocol.

2.7. Functional characterization of HepG2 cells/CYP3A4

CYP3A4 activity was measured using the P450-Glo™ Assay Kit (Promega, Wallisellen, Switzerland). Cells (HepG2 cells/wt, HepG2 cells/wt transfected with the empty vector pWpiresGFP, and HepG2 cells/CYP3A4) were seeded at 10^5 cells per cm^2 in 96-well plates and allowed to adhere overnight. After 72 h, the P450-Glo™ assay was performed according to the manufacturer's protocol using the P450-Glo™ luminogenic CYP450 substrate luciferin-BE.

2.8. Treatment of primary human hepatocytes, HepG2 cells/CYP3A4 and HepG2 cells/wt with different drugs

Primary human hepatocytes were cultured for 24 h before the addition of 20 μM rifampicin for 72 h for CYP3A4 induction. We then treated the cells with amiodarone (25 μM and 50 μM) for 24 h and determined cytotoxicty using the ToxiLight® assay (Lonza, Basel, Switzerland) as described below.

HepG2 cells/wt and HepG2 cells/CYP3A4 grown to 80–85% confluency were passaged using trypsin and 50,000 cells/well were allowed to adhere overnight in 96-well culture plates. Stock solutions of test compounds (quinidine, amitriptyline, ketoconazole and/or amiodarone) were prepared in DMSO. The reaction volume was 200 μl and DMSO concentrations never exceeded 0.2%. Cells were incubated with 0.1% Triton-X as a positive control and 0.2% DMSO as negative control. To certain incubations of HepG2 cells/wt, 20 pmol/ml CYP3A4 supersomes (HepG2 cells/CYP3A4 supersomes) or control supersomes and 1 mM of the co-factor NADPH were added. Drug treatment was performed for 24 h at 37 °C and 5% CO_2.

2.9. Cytotoxicity assay (adenylate kinase release)

The loss of cell membrane integrity is reflected in the release of adenylate kinase, which can be detected using the firefly luciferase system (ToxiLight® BioAssay Kit, Lonza, Basel, Switzerland). After 24 h of incubation in the presence of drugs, 100 μl assay buffer was added to 20 μl supernatant from drug-treated cells (concentrations indicated in the figures) and luminescence was measured after 5 min.

2.10. Quantification of amiodarone, MDEA and DDEA using HPLC

HepG2 cells/wt or HepG2 cells/CYP3A4 (450,000 cells/well) were seeded in 24-well plates and allowed to adhere overnight. Supersomes were used in certain incubations as mentioned above. After treatment with amiodarone (10, 25 or 50 μM) for 24 h, 30 μl of internal standard (IS) was added to the incubations and cells were detached using a cell scraper. Cells were lysed by freeze–thaw cycles, centrifuged at 14,000 × *g* for 10 min and the supernatant was subjected to HPLC analysis.

For quantification, we used a Merck Hitachi HPLC equipped with a column oven (L7300), an autosampler (L7200) kept at 25 °C, interface (L7000), UV-detector (L7400) operating at a wavelength of 254 nm, pump (L7100) and a Reprosil SI 80 column from Dr. Maisch GmbH (Ammerbuch, Germany). For the measurements in cell culture medium, a guard column (LiChrospher® Si60 5 μm, Merck, Germany) was used. The method was based on a validated method used for the quantification of amiodarone and its major metabolite mono-N-desethylamiodarone (MDEA) in serum developed at our institution. This method was adapted for the quantification of amiodarone, MDEA and di-N-desethylamiodarone (DDEA). The variability of the method was <10% at high and low concentrations of amiodarone, MDEA and DDEA. The mobile phase consisted of solvent A (97% methanol/3% ammonium sulphate buffer pH 8.7) and solvent B (90% methanol/10% ammonium sulphate buffer pH 8.7). The gradient was as follows: 50% A and 50% B for 5 min, increase to 100% B within 5 min and back to 50% A and 50% B within 5 min. The flow rate was 1.5 ml/min and the total run time 15 min. The injection volume was 20 μl. Quantification of amiodarone and its metabolites was by comparison to a standard curve.

2.11. Assessment of cellular metabolism

Measurement of cellular respiration was performed using a Seahorse XF24 analyzer (Seahorse Bioscience, North Billerica, MA, USA). Cells were seeded in Seahorse XF 24-well culture plates (Bucher Biotec AG, Basel, Switzerland) at 50,000 cells/well in growth medium. After treatment with amiodarone for 6 h, growth medium was replaced with 750 μl unbuffered medium (prepared by the manufacturer's instructions; Seahorse Bioscience). Cells were equilibrated to the unbuffered medium for 45 min at 37 °C in a CO_2-free incubator before being transferred to the XF24 analyzer. We measured basal OCR and ECAR, and then sequentially injected (final concentrations) 1 μM oligomycin, 1 μM carbonyl cyanide *p*-(trifluoromethoxyl)-phenyl-hydrozone (FCCP) and finally, 1 μM rotenone to assess oxidative capacity of the cells under different conditions.

2.12. Measurement of reactive oxygen species (ROS)

A fluorescence-based microplate assay [19] was used for the evaluation of oxidative stress in HepG2 cells/wt and HepG2 cells/CYP3A4 treated with the test compounds. 2′,7′-dichlorofluorescein-diacetate (DCFH-DA). Cells were simultaneously exposed to test compounds and to DCFH-DA (5 μM) and incubated for 6, 12 and 24 h. Fluorescence was measured at an excitation wavelength of 485 nm and an emission wavelength of 535 nm using a microtiter plate reader (HTS 700 Plus Bio Assay Reader; PerkinElmer, Beaconsfield, Buckinghamshire, UK) in incubations containing cells and exposure medium.

2.13. Cytochrome c release detection by fluorescence microscopy

Microscope cover glasses (diameter 13 mm; thickness 0.17 mm) were activated with (3-aminopropyl)triethoxy-silane (Tespa; Sigma No. A3648) in acetone for 5 min. 100,000 HepG2 cells/wt or HepG2 cells/CYP3A4 were seeded per well in 24-well plates and allowed to adhere on microscopy cover glasses overnight. Amiodarone (50 μM) was added to the cells for 8 h. 100 μM benzbromarone served as positive and 0.2% DMSO (DMSO ctrl) as a negative control. Cells were stained with 50 nM Mitotracker Red CMXRos (Invitrogen, Basel, Switzerland; No. M7512) for 30 min at 37 °C and crosslinked with 4% formaldehyde in PBS (Polysciences Europe GmbH, Eppelheim, Germany) for 15 min at 37 °C. Permeabilization was performed with 0.2% Triton-X-100 followed by blocking with 5% BSA (Sigma No. A2153). Immuno staining was performed using a biotinylated cytochrome *c* antibody (BioLegend, Cambridge, UK; No. 612303) at a dilution 1/20 in PBS containing 5% BSA for 45 min. Streptavidin-Alexa647 (Molecular Probes No. S32354) at a dilution 1/200 plus 1/1000 4′,6-diamidin-2′-phenylindol (DAPI) (Invitrogen, Basel, Switzerland; No. D3571) were applied in PBS containing 2.5% bovine serum albumin for 20 min. Subsequently, cells were mounted on Superfrost glass slides (Thermo Scientific, Allschwil, Switzerland) using the FluorSave reagent (Calbiochem, Läufelfingen, Switzerland; No. 345789). An Olympus IX81 inverted microscope was used for analysis in combination with the CellR software (Olympus, Volketswil, Switzerland). Images were exported as 16-bit TIFF files. ImageJ software (http://rsbweb.nih.gov/ij/) was used to convert the images to 8-bit and to create merged images and photoshop to trim images and to adjust their brightness. The opensource software ImageJ from the NIH (http://rsbweb.nih.gov/ij/) was used to quantify the signals acquired by fluorescence microscopy. The amounts of mitochondria free of cytochrome *c* (red) were determined ($n = 3$ independent determinations) and compared between control (incubation medium containing 0.2% DMSO) and treatments with amiodarone or benzbromarone.

2.14. Detection of apoptosis and necrosis using flow cytometry

200,000 cells/well were seeded in 24-well plates and allowed to adhere for 24 h before drug treatment. Drug treatment was performed for 24 h in the presence or absence of 1 μM ketoconazole (KCZ). HepG2 cells/CYP3A4 and HepG2 cells/wt were stained for 15 min with 1/20 AnnexinV-PE and 1/200 propidium iodide in a volume of 50 μl AnnexinV-binding buffer (10 mM Hepes, 150 mM NaCl, 2.5 mM $CaCl_2$, 5 mM KCl, 1 mM $MgCl_2$ in H_2O, pH 7.4). Flow cytometry was carried out on a DAKO Cyan cytometer. Benz-

Table 1
Toxicity of amiodarone on primary human hepatocytes. Cryo-preserved primary human hepatocytes (BD Gentest, Switzerland) were treated with 20 μM rifampicin for 72 h before the addition of amiodarone (25 μM or 50 μM) for 24 h. Cytotoxicity was determined using the ToxiLight® assay (Lonza, Basel/Switzerland). All incubations contained 0.2% DMSO. $N = 3$ independent experiments were performed. Data are normalized to control incubations containing no rifampicin and are expressed as mean ± SEM.

Inhibitor	No rifampicin	20 μM rifampicin
Control (0.2% DMSO)	1.00 ± 0.04	0.93 ± 0.04
Amiodarone 25 μM	0.69 ± 0.02[a]	0.75 ± 0.09
Amiodarone 50 μM	1.09 ± 0.03	1.52 ± 0.08[a,b]

[a] $p < 0.05$ versus respective control incubation.
[b] $p < 0.05$ versus respective incubation containing no rifampicin.

bromarone (100 μM) [11] and deoxycholate (200 μM) [13] were used as positive controls.

2.15. Statistical analysis

Data are presented as means ± SEM of at least three experiments. Statistical analyses were performed using Sigma Stat release 3.5 (Scientific Solutions, Pully Lausanne, Switzerland). Differences between many groups at two levels were tested by two-way analysis of variance (ANOVA) followed by Dunnet's post hoc test if the data were normally distributed. In the case of not normally distributed data, Holm–Sidak statistics was performed. Differences between groups (e.g. control versus test compound incubations in HepG2 cells/CYP3A4) were tested by one-way analysis of variance (ANOVA) followed by Dunnett's post hoc test if ANOVA showed significant differences. A p value <0.05 was considered to be significant.

3. Results

3.1. Effect of amiodarone on primary human hepatocytes

As shown in Table 1, amiodarone was toxic on primary human hepatocytes at a concentration of 50 μM and only on hepatocytes which had been treated with rifampicin. In contrast, 25 μM amiodarone appeared to have a protective effect, at least on hepatocytes which had not been treated with rifampicin.

3.2. Characterization of human CYP3A4 in stably transduced HepG2 cells

Based on the findings described above, we decided to establish HepG2 cells stably expressing CYP3A4 to be able to study the mechanisms by which CYP3A4 increases the toxicity of amiodarone in more detail. HepG2 wt cells were transduced with lentiviral supernatant (see Section 2) and the success of transduction was assessed by fluorescence-activated cell sorting (FACS) analysis. The FACS analysis revealed successfully transduced HepG2 cells, which were co-expressing EGFP and CYP3A4 (data not shown). To verify CYP3A4 overexpression, we measured mRNA expression of human CYP3A4 using RT-PCR (Fig. 1A). Quantitative real time PCR showed a >65-fold increase of CYP3A4 mRNA in the transduced cells (referred to as HepG2 cells/CYP3A4). Expectedly, transduction with the empty vector (referred to as GFP cells) showed no elevation of CYP3A4 mRNA. CYP3A4 protein expression was investigated from cellular lysates of HepG2 cells/wt, HepG2 cells/wt transfected with the empty vector pWpiresGFP or HepG2 cells/CYP3A4 (Fig. 1B). Western blot analysis revealed increased CYP3A4 protein expression exclusively in HepG2 cells/CYP3A4 (14-fold increased densitometry relative to DMSO control of HepG2 cells/wt). The functionality of the human CYP3A4 construct in HepG2 cells was assessed by measuring CYP3A4 activity using the P450-Glo™ Assay Kit as described. Qualitatively consistent with the RNA and protein expression data, HepG2 cells/CYP3A4 showed a >2.5-fold increase in CYP3A4 activity compared HepG2 cells/wt and HepG2 cells containing the empty vector pWpiresGFP (data not shown). These data indicated that HepG2 cells/CYP3A4 represented a functional, intracellular activation system for CYP3A4.

3.3. Characterization of HepG2 cells/CYP3A4 for assessing metabolic toxicity

To assess the suitability of HepG2 cells/CYP3A4 for toxicological analyses, we studied the cytotoxicity of quinidine, a compound known to be hepatotoxic [20–22]. Quinidine is metabolized by CYP3A4 [23] and the metabolites have been shown to contribute to its cytotoxicity *in vitro* [24,25]. HepG2 cells/CYP3A4 (intracellular activation) were compared to HepG2 cells co-incubated with human CYP3A4 expressing microsomes as a system with extracellular activation (HepG2 cells/CYP3A4 supersomes). Quinidine was associated with a slight cytotoxicity in HepG2 cells/wt at a concentration of 100 μM (Fig. 2A). The toxic effect was significantly increased in HepG2 cells/CYP3A4, suggesting CYP3A4-mediated generation of toxic metabolites. Ketoconazole, a well-described inhibitor of CYP3A4 [24,26], attenuated this effect, confirming the existence of toxic metabolites generated by CYP3A4. In the extracellular activation system, 100 μM quinidine also showed only slight cytotoxicity in the presence of control supersomes (Fig. 2B). Again, the effect was significantly increased

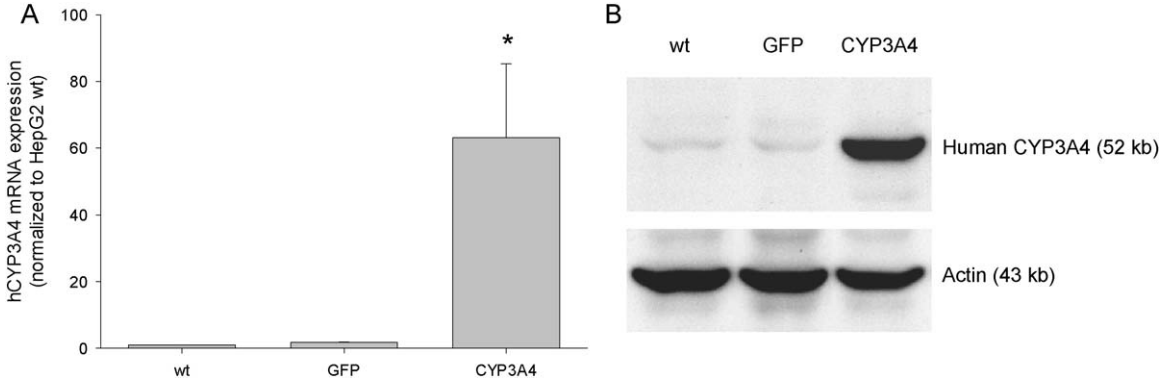

Fig. 1. Characterization of human CYP3A4 (hCYP3A4) in stably transduced HepG2 cells. (A) Characterization of hCYP3A4 mRNA expression by quantitative PCR. Data are presented as fold change relative to the expression of hCYP3A4 in wild type HepG2 cells (HepG2 cells/wt; $n = 4$). *$p < 0.01$. (B) Characterization of hCYP3A4 protein expression by Western blotting. Representative Western blot showing hCYP3A4 (52 kDa) and β-actin (43 kDa) protein expression in HepG2 cells/wt, wild type HepG2 cells expressing GFP (containing the empty vector for hCYP3A4) and HepG2 cells expressing hCYP3A4 (HepG2 cells/CYP3A4). Human CYP3A4 was detected using a polyclonal hCYP3A4 antibody. The results of the functional characterization of the HepG2 cells/CYP3A4 are given in the text. Luminescence was normalized to HepG2 cells/wt incubated with medium. Mean values ± SEM are shown of six experiments. *$p < 0.05$ versus control.

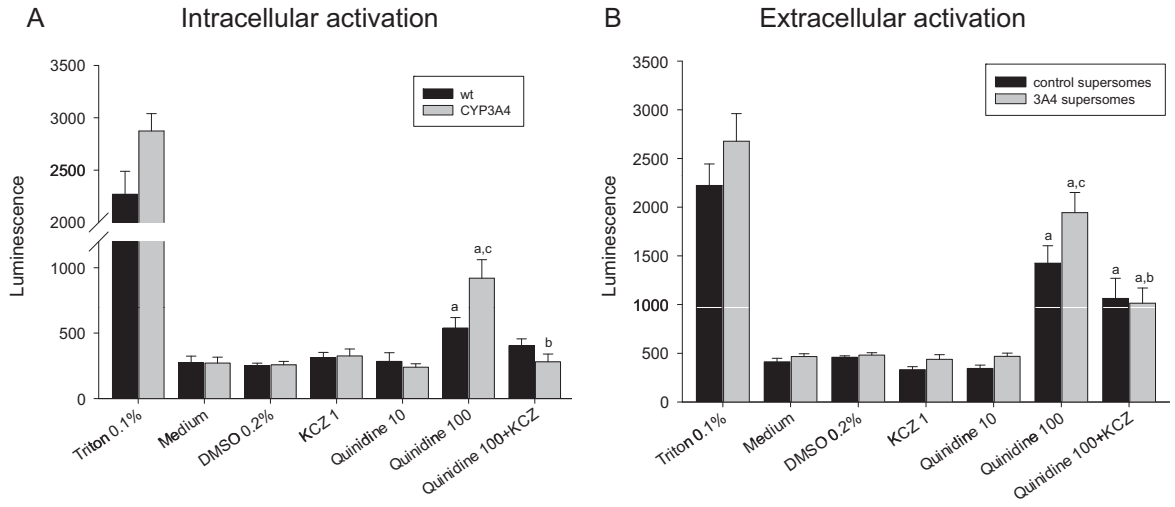

Fig. 2. Toxicological validation of HepG2 cells/CYP3A4. Toxicity of quinidine in (A) HepG2 cells/CYP3A4 compared to HepG2 cells/wt (intracellular activation) and in (B) HepG2 cells incubated with CYP3A4 supersomes (HepG2 cells/CYP3A4 supersomes) compared to HepG2 cells incubated with control supersomes (extracellular activation). Adenylate kinase release was measured after 24 h exposure to quinidine (10, 100 μM). Cell lysis with Triton-X (0.01%) served as positive control. DMSO 0.2%: medium containing 0.2% DMSO. Co-incubation with 1 μM ketoconazole (KCZ) was used to specifically inhibit CYP3A4. The cytotoxicity of quinidine is higher in the presence of CYP3A4 compared to the respective controls. The numbers following quinidine and ketoconazole (KCZ) represent concentrations (μM). Mean values ± SEM are shown of at least six independent experiments. [a] $p < 0.05$ versus control incubations containing 0.2% DMSO; [b] $p < 0.05$ versus co-incubation with ketoconazole; [c] $p < 0.05$ HepG2 cells/CYP3A4 versus HepG2 cells/wt or HepG2 cells/CYP3A4 supersomes versus control supersomes.

in incubations containing CYP3A4 supersomes and decreased in the presence of ketoconazole. CYP3A4-mediated attenuation of the cytotoxicity of amitriptyline was used as an additional characterization of the HepG2 cells/CYP3A4. Amitriptyline is metabolized by N-desalkylation and ring oxidation primarily by CYP3A4 and CYP2D6 to different metabolites [27,28]. Similar to the findings of Vignati et al. [24], cytotoxicity of amitriptyline was reduced in both systems with CYP3A4 activity compared to the control incubations, suggesting that the metabolites formed by CYP3A4 are less toxic than the mother substance (data not shown).

3.4. Toxicity of amiodarone

The toxicity of amiodarone on hepatocytes has been previously investigated [9–13,29]. Waldhauser et al. [13] proposed that the two main metabolites mono-N-desethylamiodarone (MDEA) and di-desethylamiodarone (DDEA) are at least partially responsible for the hepatocellular toxicity caused by amiodarone. The initial steps of amiodarone metabolism, N-deethylation to MDEA and DDEA, are catalyzed by CYP3A [17]. Using HepG2 cells/CYP3A4 and HepG2 cells/CYP3A4 supersomes, we aimed to investigate the metabolism of amiodarone and the toxicity of the generated metabolites in the presence of the mother substance, which reflects the clinical situation better than investigations with the individual substances. As expected, increasing amiodarone concentrations (10, 25 and 50 μM) were associated with increasing cytotoxicity in HepG2 cells/CYP3A4 (Fig. 3A). Since amiodarone failed to induce cytotoxicity in HepG2 cells/wt up to 50 μM, the toxic effect of amiodarone could be attributed to the generation of toxic metabolites by CYP3A4. Indeed, co-incubation with 1 μM ketoconazole prevented the cytotoxic effect of amiodarone in HepG2 cells/CYP3A4, confirming this assumption. In the presence

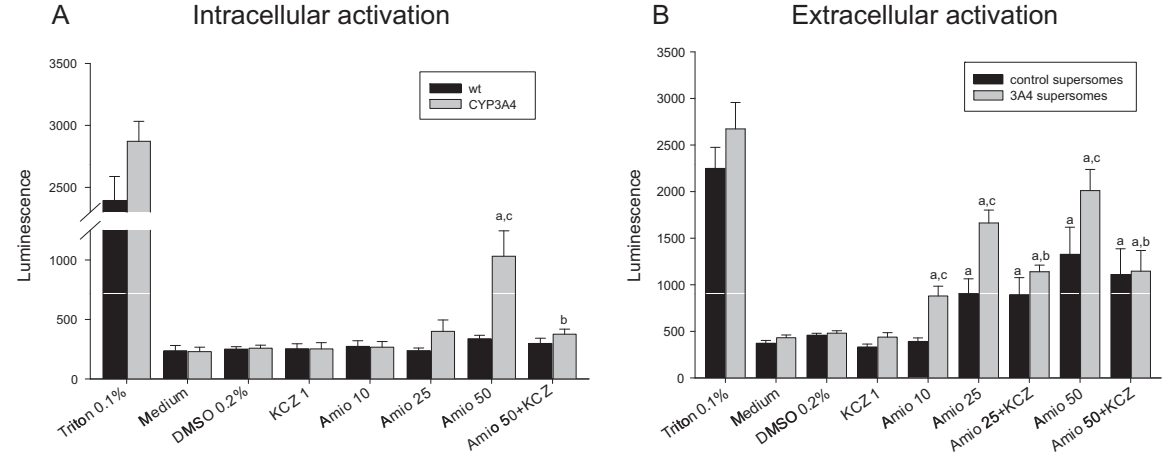

Fig. 3. Cytotoxicity of amiodarone in HepG2 cells/CYP3A4 (intracellular activation) (A) or HepG2 cells/CYP3A4 supersomes (extracellular activation) (B). Adenylate kinase release was used as a marker of cytotoxicity as described in Section 2. Triton-X (0.01%) mediated cell lysis served as a positive control and 1 μM ketoconazole (KCZ) was used as a specific CYP3A4 inhibitor. DMSO 0.2%: medium containing 0.2% DMSO. Drug treatment was performed for 24 h. Cytotoxicity of amiodarone (Amio) is higher in the presence of CYP3A4 as compared to the respective control incubations. Mean values ± SEM are shown of at least six independent experiments. [a] $p < 0.05$ versus control incubations containing 0.2% DMSO; [b] $p < 0.05$ versus co-incubation with ketoconazole; [c] $p < 0.05$ HepG2 cells/CYP3A4 versus HepG2 cells/wt or HepG2 cells/CYP3A4 supersomes versus HepG2 cells incubated with control supersomes.

Table 2
Quantification of amiodarone metabolism by HPLC. Incubation conditions are described in Section 2. Control supersomes are supersomes not containing CYP3A4. $N = 4$ independent experiments were performed. Data are presented as mean ± SEM.

Incubation time (h)	HepG2 cells/CYP3A4			HepG2 cells/wt			HepG2 cells/CYP3A4 supersomes			Control supersomes		
	Amiodarone (μM)	MDEA (μM)	DDEA (μM)	Amiodarone (μM)	MDEA (μM)	DDEA (μM)	Amiodarone (μM)	MDEA (μM)	DDEA (μM)	Amiodarone (μM)	MDEA (μM)	DDEA (μM)
(A) Incubation with 25 μM amiodarone												
0	18.7 ± 4.4	0	0	18.0 ± 3.3	0	0	19.6 ± 4.8	2.3 ± 2.3	0	24.0 ± 2.9	0	0
24	12.0 ± 1.9	7.9 ± 1.8	0.6 ± 0.6	17.2 ± 1.3	0	0	10.1 ± 1.5	15.5 ± 4.5	1.99 ± 0.7	18.4 ± 5.9	0	0
(B) Incubation with 50 μM amiodarone												
0	45.8 ± 5.2	0	0	44.7 ± 4.3	0	0	46.8 ± 8.6	1.9 ± 1.9	0.8 ± 0.8	47.3 ± 5.4	0	0
24	33.9 ± 2.6	15. ± ±2.8	2.3 ± 0.8	34.7 ± 2.1	0	0	23.4 ± 3.5	15.6 ± 3.1	3.0 ± 0.6	43.0 ± 8.5	0	0

of both CYP3A4 and control supersomes, amiodarone was associated with a concentration-dependent cytotoxicity, which was significantly more pronounced, however, in the presence of CYP3A4 supersomes (Fig. 3B). Ketoconazole significantly decreased CYP3A4-mediated cytotoxicity to the level of the incubations containing control microsomes.

3.5. Quantification of amiodarone metabolism using HPLC

The formation of the two main metabolites MDEA and DDEA was monitored by HPLC. Amiodarone, MDEA and DDEA concentrations were determined after 24 h of treatment with either 25 μM (A) or 50 μM (B) amiodarone (Table 2). The metabolites MDEA and DDEA were detected exclusively in incubations containing HepG2 cells/CYP3A4 or HepG2 cells/CYP3A4 supersomes after 24 h of amiodarone treatment. Accordingly, the amiodarone concentration decreased after an exposure of 24 h in these incubations. In contrast, HepG2 cells/wt and HepG2 cells/wt incubated with control supersomes did not generate detectable amounts of the metabolites at both amiodarone concentrations tested.

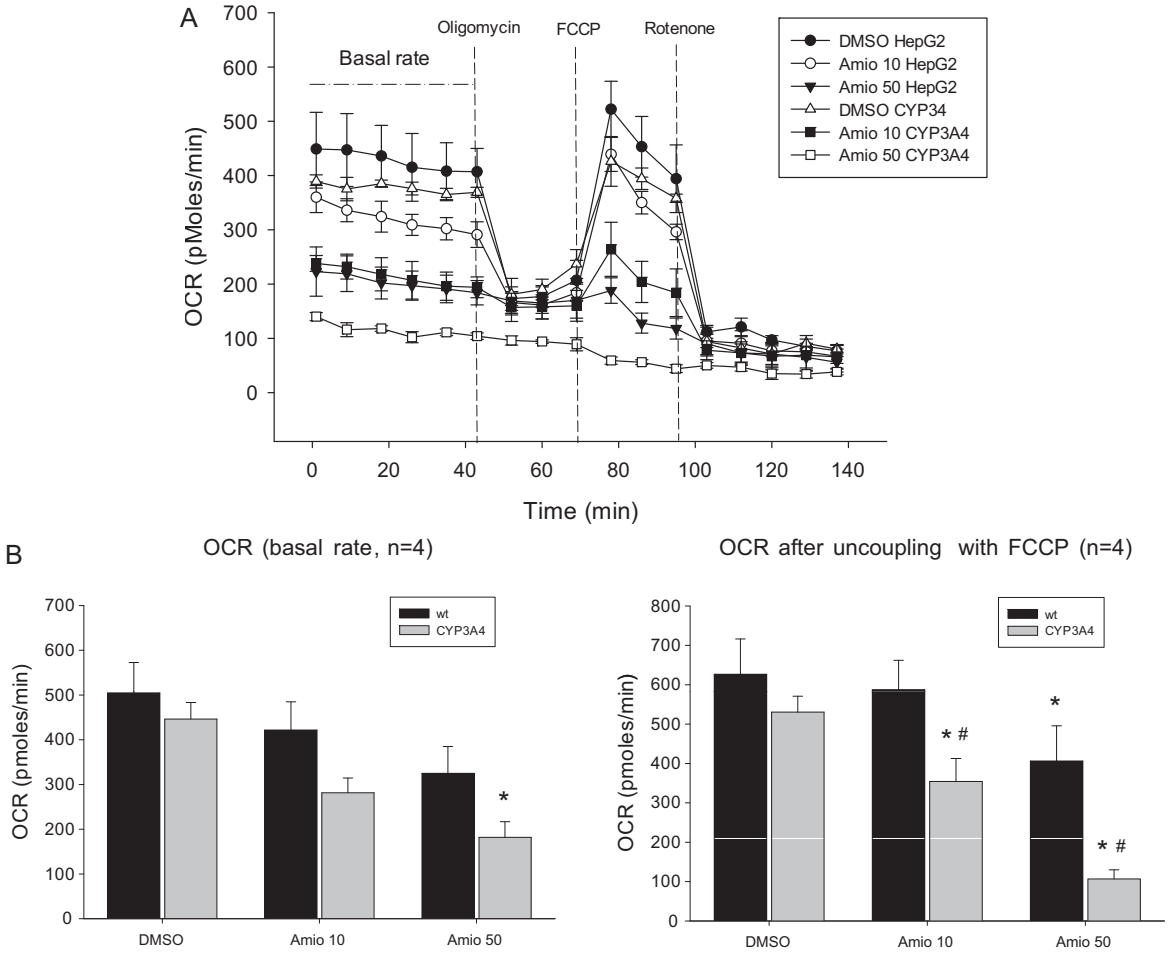

Fig. 4. Effect of amiodarone on oxygen consumption by HepG2 cells/wt and HepG2 cells/CYP3A4. Cells were treated with DMSO or amiodarone (Amio 10 μM or 50 μM) for 6 h. The XF24 analyzer was used for the measurements. (A) A representative oxygen consumption rate (OCR) experiment is shown. (B) The overall results of the basal (average at 8 min) and FCCP-stimulated (average at 78 min) OCR are shown. Amiodarone impairs OCR of HepG2 cells/wt at 50 μM. In the presence of CYP3A4, amiodarone is associated with a more pronounced decrease in the OCR compared to control incubations both at 10 and 50 μM. Similar results are obtained for FCCP-stimulated OCR. $N = 4$ independent experiments. $^{*}p < 0.05$ versus control incubations containing 0.1% DMSO; $^{\#}p < 0.05$ HepG2 cells/CYP3A4 versus HepG2 cells/wt.

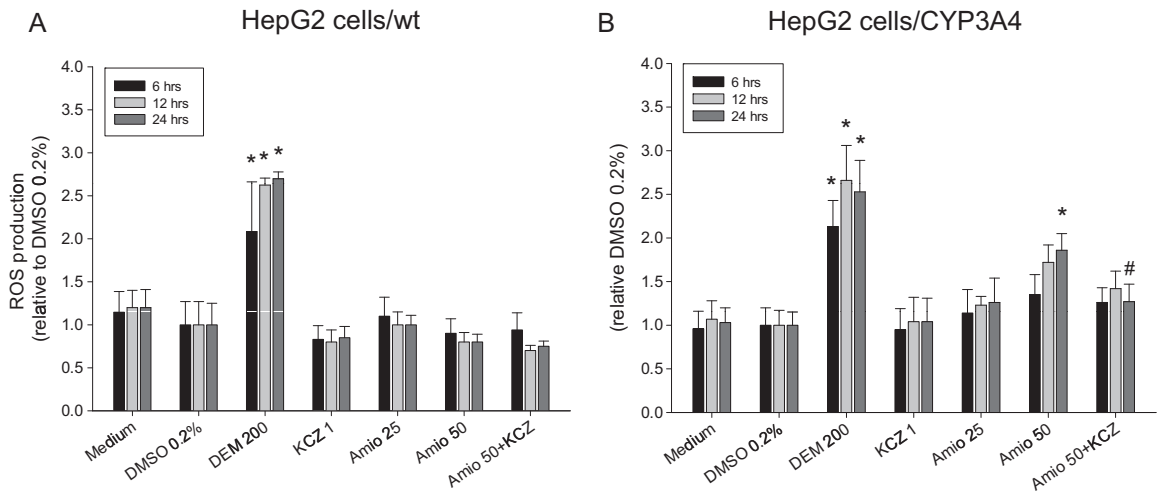

Fig. 5. ROS formation by (A) HepG2 cells/wt and (B) HepG2 cells/CYP3A4 after treatment with amiodarone (Amio) for 6, 12 and 24 h. Diethylmaleate (DEM) 200 μM served as a positive control. 1 μM ketoconazole (KCZ) was used as a specific CYP3A4 inhibitor. Results were normalized to control incubations (0.2% DMSO) and mean values ± SEM are shown of four individual experiments. 50 μM amiodarone is associated with an increase in the cellular ROS content in HepG2 cells/CYP3A4 compared to HepG2 cells/wt. $^{*}p < 0.05$ versus control incubations containing 0.2% DMSO; $^{\#}p < 0.05$ versus co-incubations with ketoconazole.

3.6. Effect of amiodarone on cellular metabolism

Cellular metabolism was assessed using the XF 24 analyzer, which is well suited for measuring the cellular oxygen consumption. As shown in Fig. 4A, cellular oxygen consumption can be measured under different conditions. Under basal conditions, cells have enough substrates for energy production (in our case mainly glucose). After inhibition of the mitochondrial F_1F_0-ATPase with oligomycin, cells exposed to uncouplers would continue to have a high oxygen uptake. After the addition of the uncoupler FCCP, the maximal activity of the mitochondrial electron transport chain under the given intracellular conditions can be assessed. Finally, after the addition of the complex I inhibitor rotenone, oxygen consumption is driven only by extramitochondrial metabolism and/or by substrates entering the mitochondrial electron transport chain at complex II (mainly succinate and partially, fatty acids).

As shown in Fig. 4B, amiodarone decreased both the basal and the FCCP-stimulated oxygen consumption by HepG2 cells/wt concentration-dependently. This was also the case in HepG2 cells/CYP3A4, but oxygen consumption was significantly lower com-

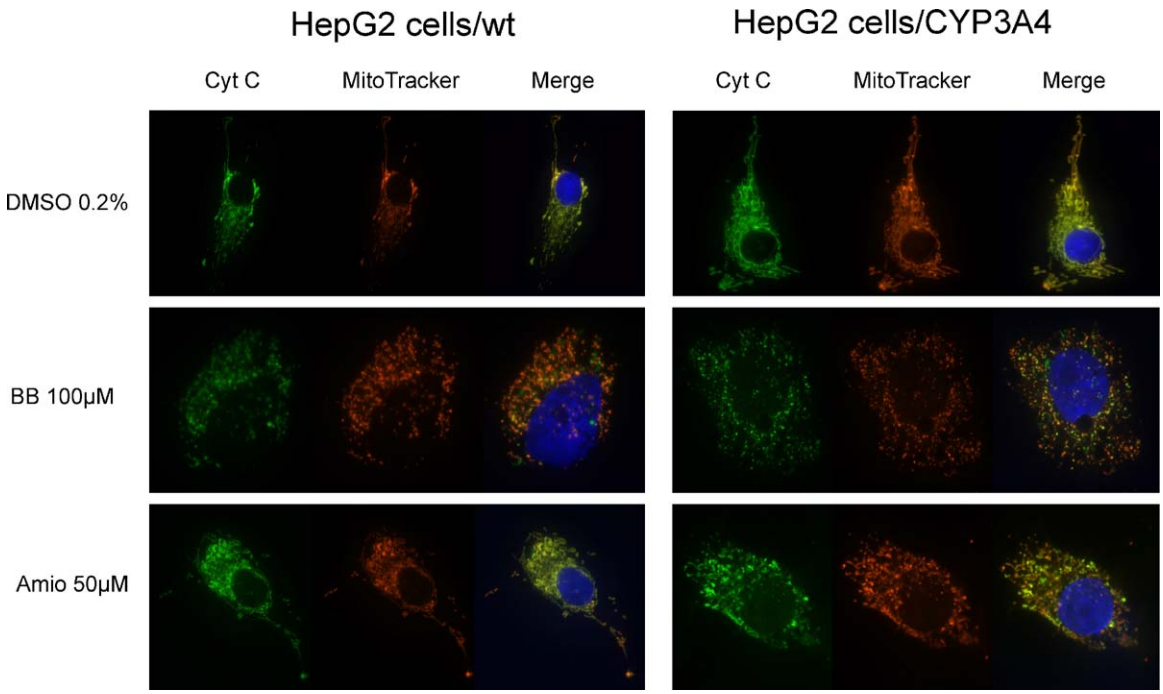

Fig. 6. Mitochondrial cytochrome *c* release detected by fluorescence microscopy. Representative images of mitochondria (MitoTracker, red), cytochrome *c* (Cyt C, green) and their co-localization (Merge, yellow) are shown. Cells were treated with 50 μM amiodarone (Amio) for 8 h and cytochrome *c* release was detected by immunofluorescence staining using a monoclonal antibody against cytochrome *c*. 0.1% DMSO (DMSO ctrl) was used as negative control and showed maximal co-localization. Benzbromarone (BB) was used as positive control and caused loss of co-localization in both HepG2 cells/CYP3A4 and HepG2 cells/wt. The area of mitochondria containing no cytochrome *c* (red color) normalized to control incubations (1.00 ± 0.40 mean ± SEM, $n = 3$ determinations) was 0.65 ± 0.08 and 5.42 ± 0.41 ($p < 0.05$ versus control) for amiodarone and benzbromarone in HepG2 cells/wt, respectively, and 2.93 ± 0.21 ($p < 0.05$ versus control and versus amiodarone in HepG2 cells/wt) and 4.68 ± 0.37 ($p < 0.05$ versus control) in HepG2 cells/CYP3A4, respectively.

pared to HepG2 cells/wt at both amiodarone concentrations. Uncoupling associated with amiodarone and/or amiodarone metabolites could not be detected and rotenone almost completely blocked cellular oxygen consumption in both cell types investigated. The results indicate that amiodarone inhibits the function of the mitochondrial electron transport chain and that this inhibition is accentuated in the presence of CYP3A4.

3.7. ROS production associated with amiodarone and/or amiodarone metabolites

ROS formation can be a consequence of the inhibition of the electron transport chain [11], which has been demonstrated for amiodarone as well as for the two metabolites MDEA and DDEA in isolated rat hepatocytes [13]. We therefore investigated whether there was a difference in ROS formation by HepG2 cells/CYP3A4 compared to HepG2 cells/wt incubated with amiodarone (Fig. 5). HepG2 cells/CYP3A4 and HepG2 cells/wt were treated with amiodarone (25 or 50 μM) for 6, 12 and 24 h and ROS production was assessed as described in Section 2. In HepG2 cells/CYP3A4, amiodarone was associated with a concentration and time-dependent increase in ROS formation, reaching significance for 24 h incubation at 50 μM amiodarone (Fig. 5A). In contrast, HepG2 cells/wt cultured at the same conditions did not show an increase in ROS production (Fig. 5B). Co-incubation with 1 μM ketoconazole attenuated ROS production in HepG2 cells/CYP3A4.

3.8. Mitochondrial damage and cytochrome c release caused by amiodarone

Production of ROS can be associated with mitochondrial disruption, leading to a release of cytochrome *c* into the cytoplasm, a key event in mitochondrial dependent apoptosis and/or necrosis [11,30]. We therefore investigated mitochondrial damage and leakage of cytochrome *c* by fluorescence microscopy. For this, we labeled mitochondria with the fluorescent MitoTracker reagent and cytochrome *c* with a monoclonal antibody. As shown in Fig. 6, 50 μM amiodarone induced mitochondrial damage and subsequent release of cytochrome *c* in HepG2 cells/CYP3A4 (as evidenced by a loss of co-localization of mitochondria and cytochrome *c* in the merged picture). In contrast, HepG2 cells/wt exhibited strict co-localization of mitochondria and cytochrome *c* upon amiodarone treatment, demonstrating again the importance of CYP3A4 for amiodarone-associated toxicity. Benzbromarone (100 μM), a previously described mitochondrial toxin [11] used as a positive control, induced mitochondrial damage and cytochrome *c* release in both, HepG2 cells/wt and HepG2 cells/CYP3A4.

3.9. Determination of amiodarone-induced apoptosis and/or necrosis

The ability of metabolized amiodarone to induce early or late stages of apoptosis was investigated using AnnexinV/propidium iodide staining, which is often used to distinguish between these two possibilities [11,30]. HepG2 cells/CYP3A4 showed a significant increase in late apoptosis/necrosis after 24 h of amiodarone treatment (25 and 50 μM) compared to HepG2 cells/wt (Fig. 7B). Co-incubation with 1 μM ketoconazole attenuated the effect. Interestingly, there was no significant increase in the percentage of early apoptotic cells (Fig. 7A), which is in line with previous investigations using 100 μM of amiodarone, MDEA or DDEA [13].

4. Discussion

To address the question whether a high activity of CYP3A4 contributes to the hepatic toxicity of amiodarone, we constructed two cellular systems allowing to investigate amiodarone metabolism and toxicity simultaneously. As a proof of concept, we first showed that CYP induction with rifampicin increases the toxicity of amiodarone on human primary hepatocytes. Next, we established a system with intracellular amiodarone metabolism (HepG2 cells overexpressing hCYP3A4) and a system with extracellular metabolism of amiodarone (HepG2 cells co-incubated with CYP3A4 supersomes). We characterized the HepG2 cells overexpressing hCYP3A4 (HepG2 cells/CYP3A4) by measuring the expression of CYP3A4 on the mRNA and protein level and by the determination of the CYP3A4 activity. While HepG2 cells/CYP3A4 had a more than 10-fold increase in the expression of CYP3A4 mRNA and protein compared to HepG2 cells/wt, the activity of CYP3A4 (determined using the P450-Glo™ assay) was doubled. We investigated the activity of CYP3A4 also by the formation of the amiodarone metabolites MDEA and DDEA using HPLC. In the presence of HepG2 cells/wt, no metabolite formation was

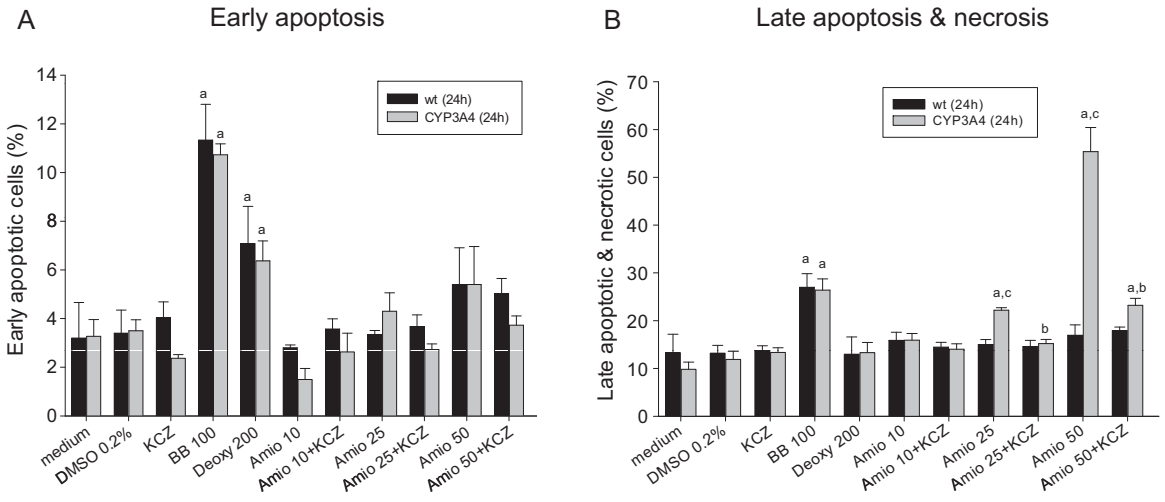

Fig. 7. Determination of apoptosis and/or necrosis following amiodarone treatment. Apoptosis was assessed using fluorescence labeled AnnexinV and propidium iodide followed by flow cytometry analysis. 200 μM deoxycholate (Deoxy) was used as a positive control for early apoptosis and 100 μM benzbromarone (BB) as a positive control for early and late apoptosis/necrosis [11]. 1 μM ketoconazole (KCZ) was used as a specific CYP3A4 inhibitor. 25 and 50 μM amiodarone are associated with late apoptosis only in HepG2 cells/CYP3A4 but not in HepG2 cells/wt. Mean values ± SEM of three independent experiments are shown. [a] $p < 0.05$ versus control incubations containing 0.2% DMSO; [b] $p < 0.05$ versus co-incubation with ketoconazole; [c] $p < 0.05$ HepG2 cells/CYP3A4 versus HepG2 cells/wt.

detectable. In contrast, HepG2 cells/CYP3A4 metabolized approximately 40% of amiodarone during 24 h, demonstrating the presence of functional CYP3A4.

To further validate the two activation systems, we used the test compound quinidine, which requires metabolic activation through CYP3A4 to manifest cytotoxicity [24,25]. 3-Hydroxyquinidine is the main toxic metabolite of quinidine, which can cause heart, renal and/or hepatic injury [31]. Quinidine showed a dose-dependent cytotoxicity in both cell systems studied when compared to the corresponding control incubations (Fig. 2A). The role of CYP3A4 in cytotoxicity of quinidine could clearly be demonstrated by the addition of ketoconazole, which blocks CYP3A4 activity [24,26] and significantly decreased cytotoxicity associated with quinidine.

After having validated our systems, we next studied the toxicity of amiodarone in HepG2 cells/CYP3A4 and HepG2 cells/CYP3A4 supersomes [17]. Since it is known from previous studies that both N-desethyl-metabolites are cytotoxic [13,14,25], we were interested to investigate whether the generation of these metabolites could be a reason for amiodarone-associated hepatotoxicity. After incubation for 24 h, amiodarone clearly showed a higher toxicity in HepG2 cells/CYP3A4 and HepG2 cells co-incubated with CYP3A4 supersomes (HepG2 cells/CYP3A4 supersomes) compared to the corresponding control incubations not containing CYP3A4. Again, ketoconazole significantly reduced cytotoxicity of amiodarone in these two systems. In addition, we detected the generation of MDEA and DDEA exclusively in HepG2 cells/CYP3A4 and HepG2 cells/CYP3A4 supersomes, whereas HepG2 cells/wt or HepG2 cells incubated with control supersomes failed to produce these metabolites. These results indicated that MDEA and/or DDEA were responsible for most of the cytotoxicity of amiodarone in our systems. Furthermore, cytotoxicity was not reduced with extracellular compared to intracellular generation of the metabolites, indicating the toxic metabolites are stable enough to the penetrate plasma membrane and probably also cellular organelles such as mitochondria.

The exact mechanisms leading to cytotoxicity of amiodarone are not completely understood, but are assumed to involve mitochondrial toxicity of the parent compound and/or of the metabolites as suggested by several *in vivo* [10] and *in vitro* studies [9,11–14,29]. HepG2 cells overexpressing hCYP3A4 offered an excellent possibility to study the significance of the amiodarone metabolites formed for the different steps involved in the suggested mechanism of amiodarone cytotoxicity.

As expected, the cellular oxygen consumption, which, under the conditions used, was mainly reflecting the function of the mitochondrial electron transport chain (Fig. 4A), was clearly lower in HepG2 cells/CYP3A4 compared to HepG2 cells/wt. Interestingly, 50 μM amiodarone was associated with a clear reduction in oxygen consumption also in HepG2 cells/wt, whereas this amiodarone concentration was not cytotoxic in the same cellular system (Fig. 3A). This illustrates that mitochondrial metabolism may be more sensitive than cytotoxicity for assessing cellular effects of toxicants, possibly because HepG2 cells can switch between oxidative and glycolytic metabolism depending on the cellular environment such as the presence of toxicants [32].

Since an impaired activity of the respiratory chain can be associated with increased ROS production [11] and since increased ROS production has already been shown in cells exposed to MDEA or DDEA [13], we next assessed cellular ROS production. Cellular ROS concentrations were increased only in HepG2 cells/CYP3A4 at 50 μM amiodarone, suggesting that the mitochondrial defense mechanisms for ROS accumulation were sufficient at lower amiodarone concentrations and in HepG2 cells/wt (Fig. 4).

Since increased cellular ROS concentrations are associated with mitochondrial cytochrome *c* release and apoptosis [11,30,33,34], we assessed these events. Mitochondrial cytochrome *c* release and induction of apoptosis and/or necrosis were much more pronounced in HepG2 cells/CYP3A4 exposed to amiodarone (Figs. 6 and 7), compared to HepG2 cells/wt. Again, the importance of CYP3A4 was confirmed for both cytochrome *c* release and induction of apoptosis using ketoconazole as an inhibitor of CYP3A4 mediated metabolism of amiodarone.

The results of the current study support therefore the hypothesis that amiodarone is a mitochondrial toxin and that its hepatocellular toxicity is mainly associated with the metabolites MDEA and DDEA. They also demonstrate the value of HepG2 cells/CYP3A4 for toxicological studies, since they are not only producing CYP3A4-dependent metabolites, but contain also important toxicological effector systems [11,13]. Since treatment with rifampicin was associated with a significant increase in the cytotoxicity of amiodarone in primary human hepatocytes, our *in vitro* observations may also be clinically relevant.

Acknowledgements

We would like to thank Liliane Todesco for initial help with the HPLC. The study was supported by a grant from the Swiss National Science Foundation [31003A-112483 to S.K.].

References

[1] Mason JW. Amiodarone. New Engl J Med 1987;316:455–66.
[2] Harjai KJ, Licata AA. Effects of amiodarone on thyroid function. Ann Intern Med 1997;126:63–73.
[3] Jessurun GA, Boersma WG, Crijns HJ. Amiodarone-induced pulmonary toxicity. Predisposing factors, clinical symptoms and treatment. Drug Saf 1998;18:339–44.
[4] Pitcher WD. Amiodarone pulmonary toxicity. Am J Med Sci 1992;303:206–12.
[5] Pollak PT. Clinical organ toxicity of antiarrhythmic compounds: ocular and pulmonary manifestations. Am J Cardiol 1999;84:37R–45R.
[6] Lewis JH, Mullick F, Ishak KG, Ranard RC, Ragsdale B, Perse RM, et al. Histopathologic analysis of suspected amiodarone hepatotoxicity. Hum Pathol 1990;21:59–67.
[7] Lewis JH, Ranard RC, Caruso A, Jackson LK, Mullick F, Ishak KG, et al. Amiodarone hepatotoxicity: prevalence and clinicopathologic correlations among 104 patients. Hepatology 1989;9:679–85.
[8] Morse RM, Valenzuela GA, Greenwald TP, Eulie PJ, Wesley RC, McCallum RW. Amiodarone-induced liver toxicity. Ann Intern Med 1988;109:838–40.
[9] Fromenty B, Fisch C, Berson A, Letteron P, Larrey D, Pessayre D. Dual effect of amiodarone on mitochondrial respiration. Initial protonophoric uncoupling effect followed by inhibition of the respiratory chain at the levels of complex I and complex II. J Pharmacol Exp Ther 1990;255:1377–84.
[10] Fromenty B, Fisch C, Labbe G, Degott C, Deschamps D, Berson A, et al. Amiodarone inhibits the mitochondrial beta-oxidation of fatty acids and produces microvesicular steatosis of the liver in mice. J Pharmacol Exp Ther 1990;255:1371–6.
[11] Kaufmann P, Torok M, Hanni A, Roberts P, Gasser R, Krahenbuhl S. Mechanisms of benzarone and benzbromarone-induced hepatic toxicity. Hepatology 2005;41:925–35.
[12] Spaniol M, Bracher R, Ha HR, Follath F, Krahenbuhl S. Toxicity of amiodarone and amiodarone analogues on isolated rat liver mitochondria. J Hepatol 2001;35:628–36.
[13] Waldhauser KM, Torok M, Ha HR, Thomet U, Konrad D, Brecht K, et al. Hepatocellular toxicity and pharmacological effect of amiodarone and amiodarone derivatives. J Pharmacol Exp Ther 2006;319:1413–23.
[14] Bolt MW, Card JW, Racz WJ, Brien JF, Massey TE. Disruption of mitochondrial function and cellular ATP levels by amiodarone and N-desethylamiodarone in initiation of amiodarone-induced pulmonary cytotoxicity. J Pharmacol Exp Ther 2001;298:1280–9.
[15] Flanagan RJ, Storey GC, Holt DW, Farmer PB. Identification and measurement of desethylamiodarone in blood plasma specimens from amiodarone-treated patients. J Pharm Pharmacol 1982;34:638–43.
[16] Ha HR, Bigler L, Wendt B, Maggiorini M, Follath F. Identification and quantitation of novel metabolites of amiodarone in plasma of treated patients. Eur J Pharm Sci 2005;24:271–9.
[17] Fabre G, Julian B, Saint-Aubert B, Joyeux H, Berger Y. Evidence for CYP3A-mediated N-deethylation of amiodarone in human liver microsomal fractions. Drug Metab Dispos 1993;21:978–85.
[18] Salmon P, Oberholzer J, Occhiodoro T, Morel P, Lou J, Trono D. Reversible immortalization of human primary cells by lentivector-mediated transfer of specific genes. Mol Ther 2000;2:404–14.
[19] Wang H, Joseph JA. Quantifying cellular oxidative stress by dichlorofluorescein assay using microplate reader. Free Radic Biol Med 1999;27:612–6.

[20] Handler SD, Hirsch NR, Haas K, Davidson FZ. Quinidine hepatitis. Arch Intern Med 1975;135:871–2.
[21] Koch MJ, Seeff LB, Crumley CE, Rabin L, Burns WA. Quinidine hepatotoxicity. A report of a case and review of the literature. Gastroenterology 1976;70:1136–40.
[22] Slezak P. Quinidine hepatotoxicity. Med J Aust 1981;1:139.
[23] Foti RS, Rock DA, Wienkers LC, Wahlstrom JL. Selection of alternative CYP3A4 probe substrates for clinical drug interaction studies using in vitro data and in vivo simulation. Drug Metab Dispos 2010;38:981–7.
[24] Vignati L, Turlizzi E, Monaci S, Grossi P, Kanter R, Monshouwer M. An in vitro approach to detect metabolite toxicity due to CYP3A4-dependent bioactivation of xenobiotics. Toxicology 2005;216:154–67.
[25] Wang K, Shindoh H, Inoue T, Horii I. Advantages of in vitro cytotoxicity testing by using primary rat hepatocytes in comparison with established cell lines. J Toxicol Sci 2002;27:229–37.
[26] Zahno A, Brecht K, Bodmer M, Bur D, Tsakiris DA, Krahenbuhl S. Effects of drug interactions on biotransformation and antiplatelet effect of clopidogrel in vitro. Br J Pharmacol 2010;161:393–404.
[27] Breyer-Pfaff U. The metabolic fate of amitriptyline, nortriptyline and amitriptylinoxide in man. Drug Metab Rev 2004;36:723–46.
[28] Wen B, Ma L, Zhu M. Bioactivation of the tricyclic antidepressant amitriptyline and its metabolite nortriptyline to arene oxide intermediates in human liver microsomes and recombinant P450s. Chem Biol Interact 2008;173:59–67.
[29] Waldhauser KM, Brecht K, Hebeisen S, Ha HR, Konrad D, Bur D, et al. Interaction with the hERG channel and cytotoxicity of amiodarone and amiodarone analogues. Br J Pharmacol 2008;155:585–95.
[30] Kaufmann P, Torok M, Zahno A, Waldhauser KM, Brecht K, Krahenbuhl S. Toxicity of statins on rat skeletal muscle mitochondria. Cell Mol Life Sci 2006;63:2415–25.
[31] Jaeger A, Sauder P, Kopferschmitt J, Flesch F. Clinical features and management of poisoning due to antimalarial drugs. Med Toxicol Adv Drug Exp 1987;2:242–73.
[32] Loiseau D, Morvan D, Chevrollier A, Demidem A, Douay O, Reynier P, et al. Mitochondrial bioenergetic background confers a survival advantage to HepG2 cells in response to chemotherapy. Mol Carcinog 2009;48:733–41.
[33] Green DR, Reed JC. Mitochondria and apoptosis. Science 1998;281:1309–12.
[34] Leist M, Single B, Castoldi AF, Kuhnle S, Nicotera P. Intracellular adenosine triphosphate (ATP) concentration: a switch in the decision between apoptosis and necrosis. J Exp Med 1997;185:1481–6.